

Supplemental Information

Manipulation of Nephron-Patterning Signals Enables Selective Induction of Podocytes from Human Pluripotent Stem Cells

Yasuhiro Yoshimura, Atsuhiko Taguchi, Shunsuke Tanigawa, Junji Yatsuda, Tomomi Kamba, Satoru Takahashi, Hidetake Kurihara, Masashi Mukoyama, and Ryuichi Nishinakamura

SUPPLEMENTAL TABLE OF CONTENTS

Supplemental Figures 1 – 10

Supplemental Figure 1. Antibody-based NPC purification from mouse embryonic kidney.

Supplemental Figure 2. A low concentration of CHIR supports nephron epithelialization after transient NPC induction.

Supplemental Figure 3. NPCs require optimal concentration and duration of CHIR treatment for MET induction.

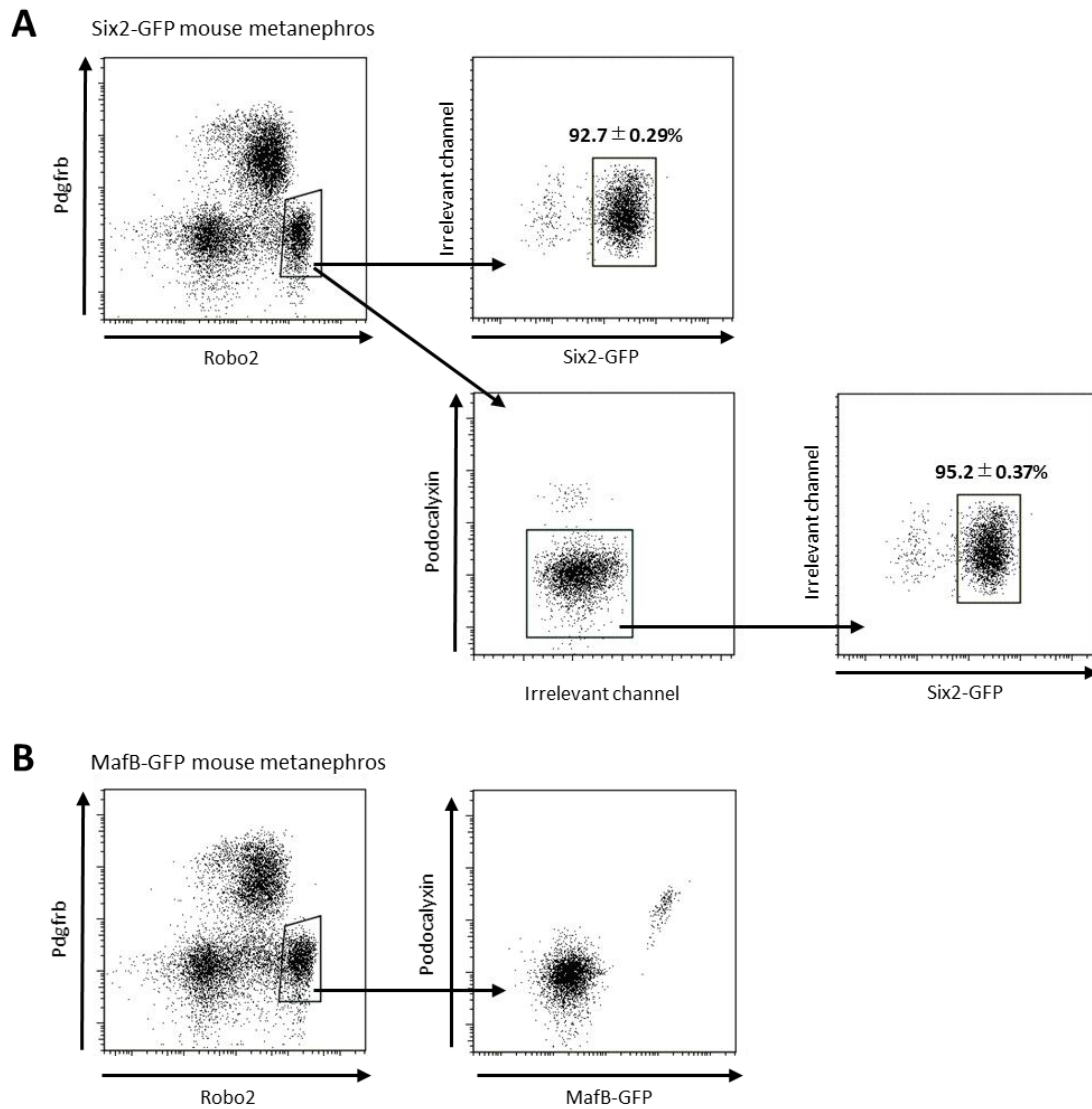
Supplemental Figure 4. Effects of growth factors or small molecules in the PA-to-RV step on podocyte differentiation.

Supplemental Figure 5. Effects of growth factors or small molecules after the RV step on podocyte differentiation.

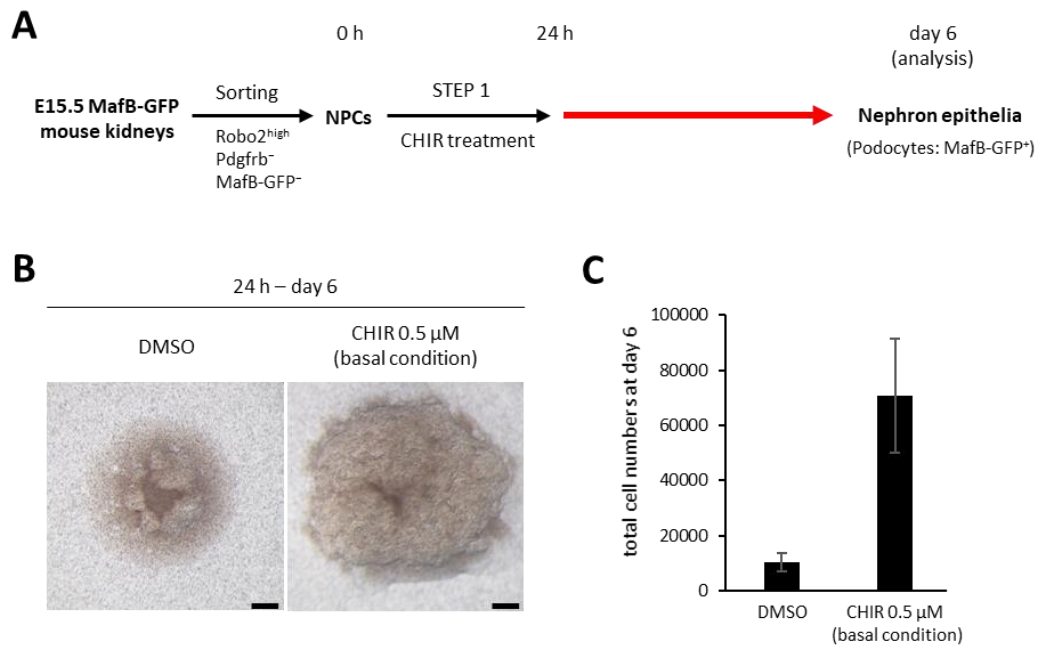
1

Supplemental Figure 6. Establishment of a selective podocyte induction method from hiPSC-derived NPCs.

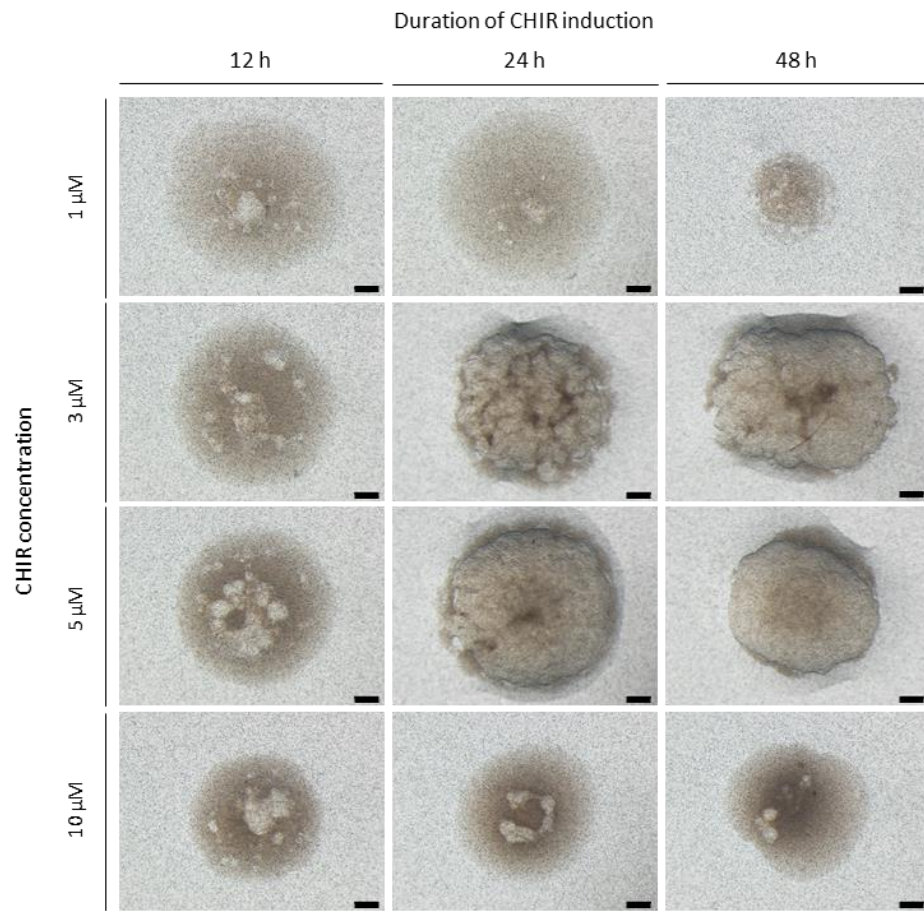
Supplemental Figure 7. Time-course analyses of differentiating cells in the podocyte induction protocol compared with the control protocol.



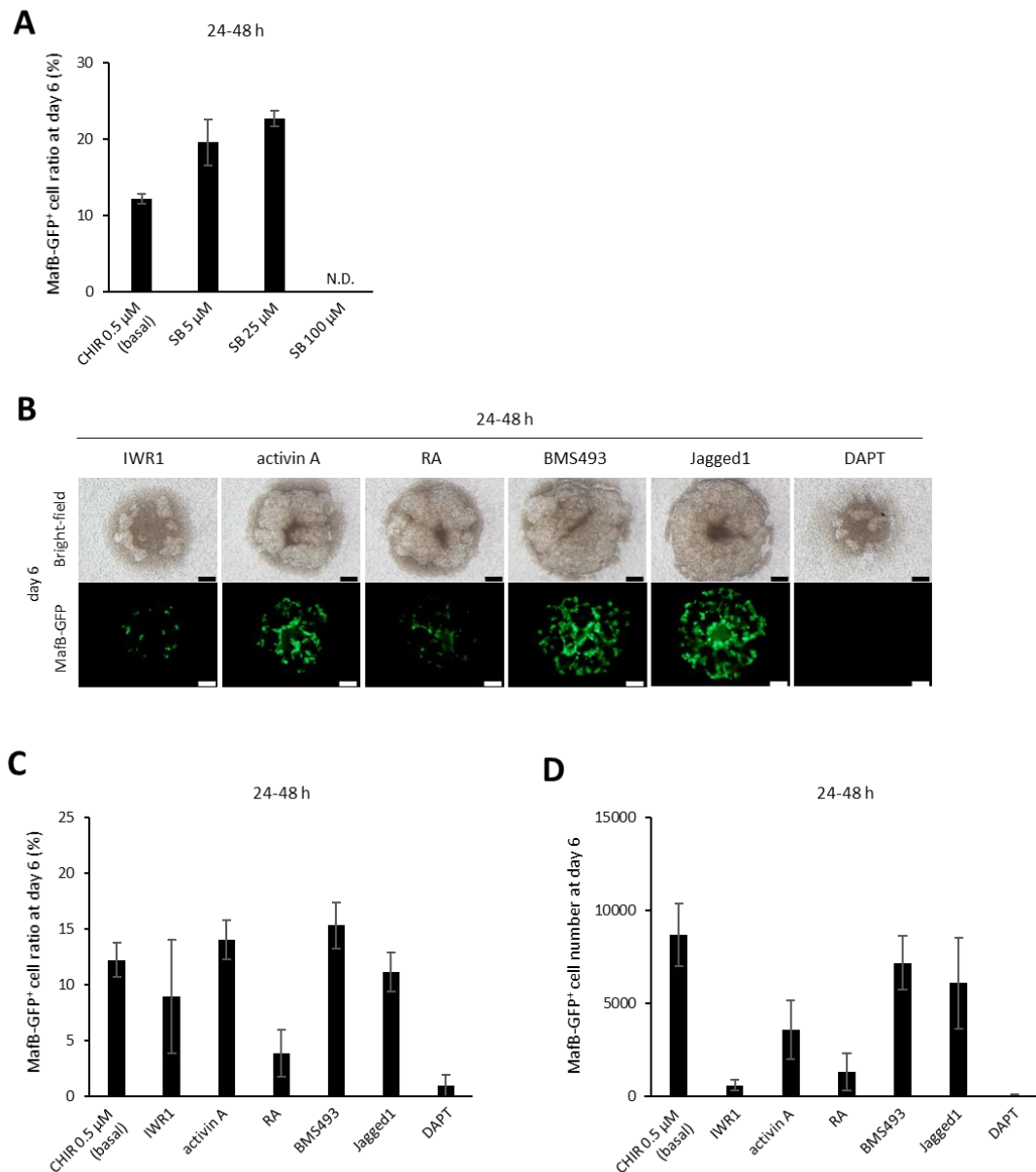
Supplemental Figure 1. Antibody-based NPC purification from mouse embryonic kidney. (A) Flow cytometry analysis of E15.5 Six2-GFP embryonic kidneys with anti-Robo2, anti-Pdgfrb, and anti-Podocalyxin antibodies (n=3). For enrichment of nephron progenitor cells (NPCs), the Podocalyxin⁺ fraction is gated out to eliminate differentiated podocytes, which also reside in the Robo2^{high}/Pdgfrb⁻ fraction. The percentages of cells in the black squares are shown (averaged from three separate experiments). (B) Flow cytometry analysis of E15.5 MafB-GFP embryonic kidneys with anti-Robo2, anti-Pdgfrb, and anti-Podocalyxin antibodies (n=3). Data are shown as means \pm SEM.



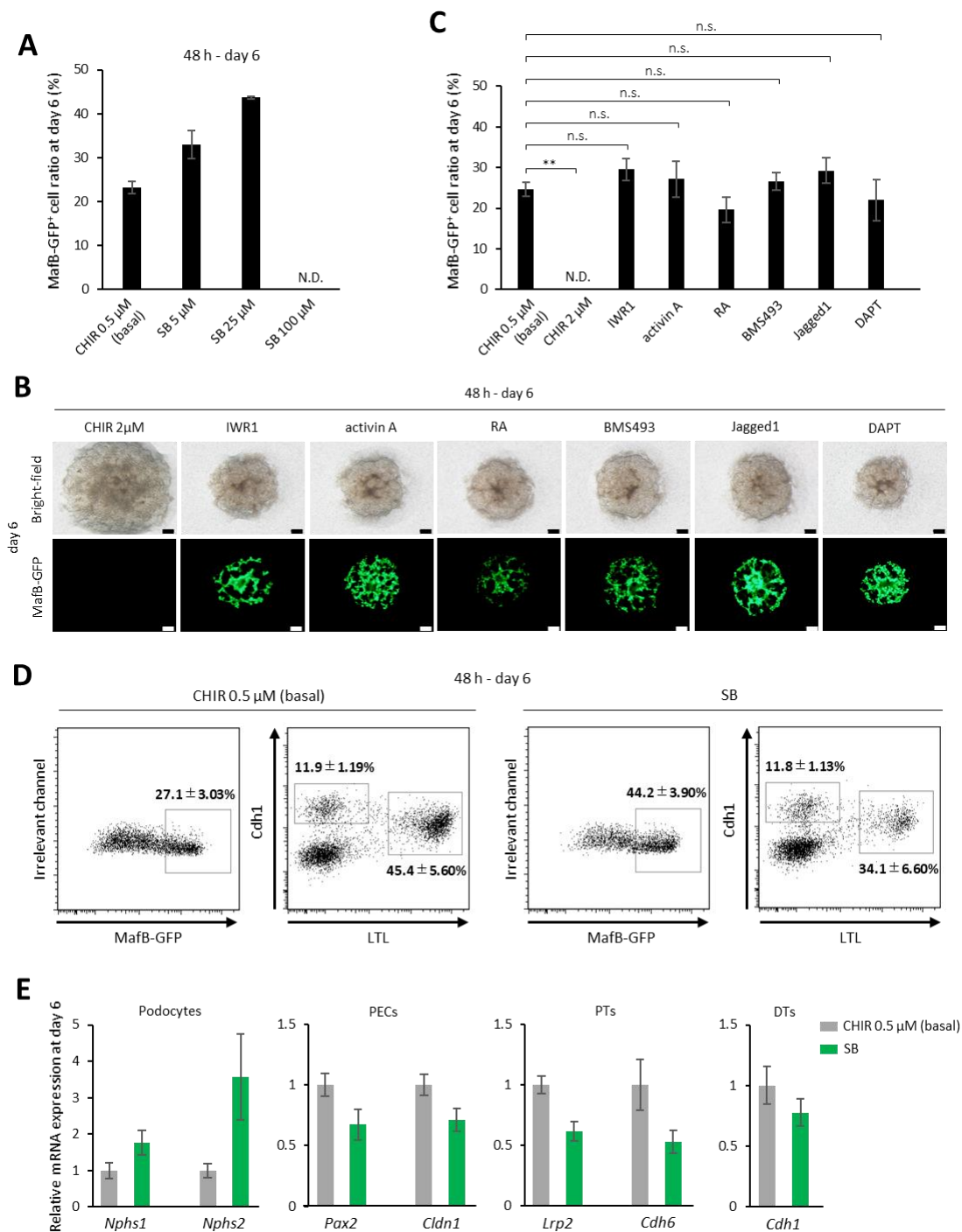
Supplemental Figure 2. A low concentration of CHIR supports nephron epithelialization after transient NPC induction. (A) Schematic representation of the experiment examining the differentiation step after the initial CHIR99021 (CHIR) treatment of NPCs. (B) Bright-field images of induced nephron epithelia at day 6 in each condition (n=3). Scale bars, 200 μm. (C) Cell numbers in induced nephron epithelia at day 6 in each condition (n=3). Data are shown as means ± SEM.



Supplemental Figure 3. NPCs require optimal concentration and duration of CHIR treatment for MET induction. Bright-field images of induced tissues at day 6 in each condition are shown (n=3). Scale bars, 200 μ m.



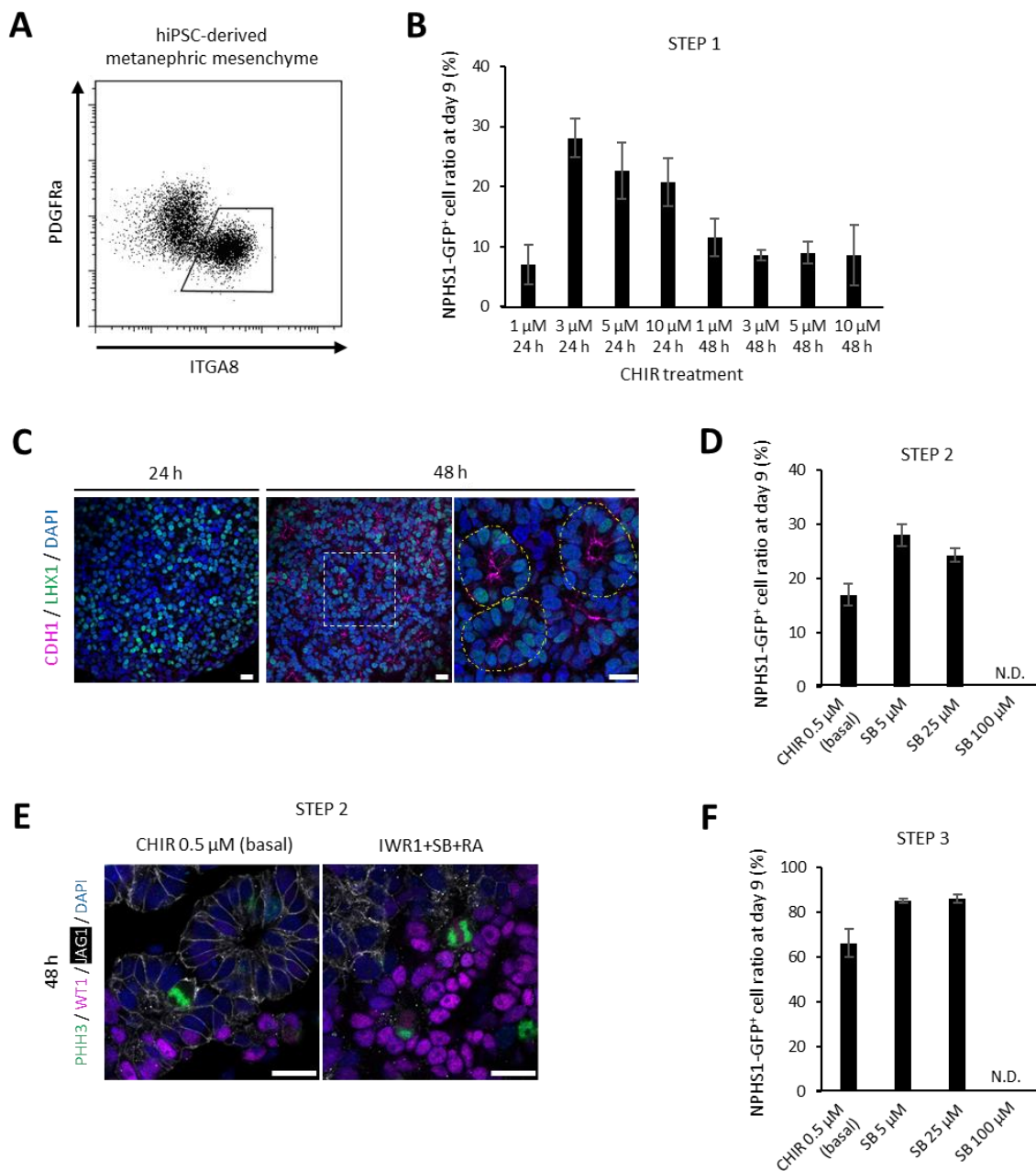
Supplemental Figure 4. Effects of growth factors or small molecules in the PA-to-RV step on podocyte differentiation. (A) Results of flow cytometry analyses at day 6 by modulating the concentration of SB431542 (SB) in the pretubular aggregate (PA)-to-renal vesicle (RV) step (n=3). basal, basal condition. N.D., not detected. (B) Bright-field (upper panels) and fluorescence (MafB-GFP, lower panels) images of induced tissues at day 6 by modulating the differentiation factors in the PA-to-RV step (n=3). RA, retinoid acid; DAPT, γ -secretase inhibitor. Scale bars, 200 μ m. (C) Results of flow cytometry analyses at day 6 by modulating the differentiation factors in the PA-to-RV step (n=3). (D) Estimated podocyte numbers in induced tissues at day 6 by modulating the differentiation factors in the PA-to-RV step. MafB-GFP⁺ cell numbers were obtained by multiplying the percentages of MafB-GFP⁺ cells and the total cell numbers in the induced tissues (n=3). Data are shown as means \pm SEM.



Supplemental Figure 5. Effects of growth factors or small molecules after the RV step on podocyte differentiation. (A) Results of flow cytometry analyses at day 6 by modulating the concentration of SB after the RV step (n=3). N.D., not detected. (B) Bright-field (upper panels) and fluorescence (MafB-GFP, lower panels) images of induced tissues at day 6 by modulating the differentiation factors after the RV step (n=3). Scale bars, 200 μm. (C) Results of flow cytometry analyses at day 6 by modulating the differentiation factors after the RV step (n=3). N.D., not detected.

(legend continued on next page)

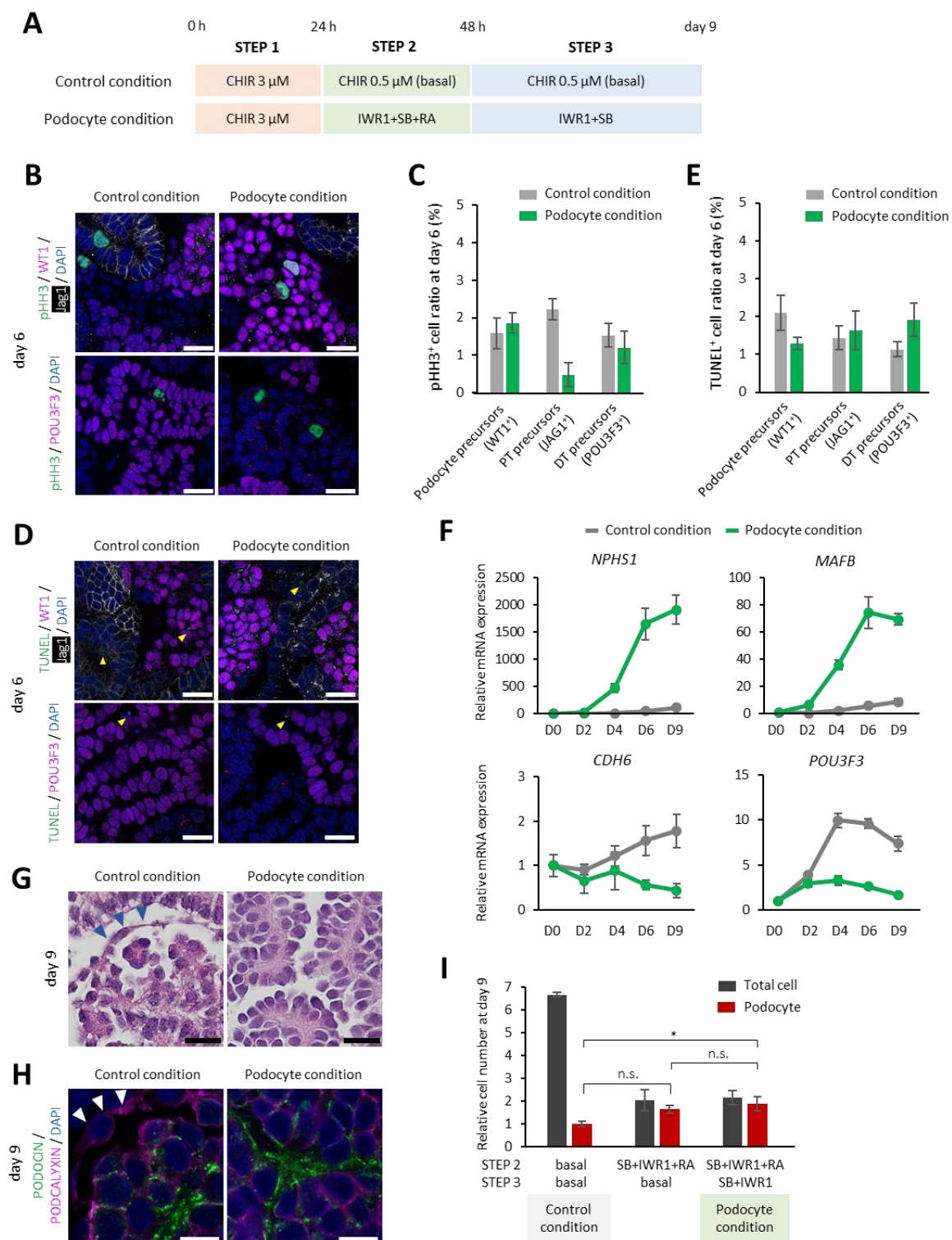
****P<0.01, n.s., not significant, Student's *t*-test.** (D) Flow cytometry analyses of induced tissues at day 6 in each condition with anti-LTL and anti-Cdh1 antibodies as well as endogenous MafB-GFP signals. The percentages of the cells in the black squares are shown (averaged from four separate experiments) (n=4). SB (25 μ M). (E) Relative expression levels of segment-specific marker genes to β -actin expression at day 6 (n=3). PECs, parietal epithelial cells; PTs, proximal tubules; DTs, distal tubules. Data are shown as means \pm SEM.



Supplemental Figure 6. Establishment of a selective podocyte induction method from hiPSC-derived NPCs. (A) Flow cytometry analysis of hiPSC-derived metanephric mesenchyme with anti-ITGA8 and anti-Pdgfra antibodies (n=5). NPCs were purified as an ITGA8⁺/Pdgfra⁻ population. (B) Results of flow cytometry analyses at day 9 by modulating the concentration and duration of the initial CHIR treatment (STEP 1) (n=4). (C) Immunostaining for LHX1 (PA and RV marker) and CDH1 (RV marker), and nuclear DAPI staining in differentiating cells at the indicated time points (n=3). The right panel shows a higher magnification image of the white dashed square in the middle panel. The epithelial vesicles are outlined by yellow dashed lines. Scale bars, 20 μ m. (D) Results of flow cytometry analyses at day 9 by modulating the concentration of SB in the PA-to-RV step (STEP 2)

(legend continued on next page)

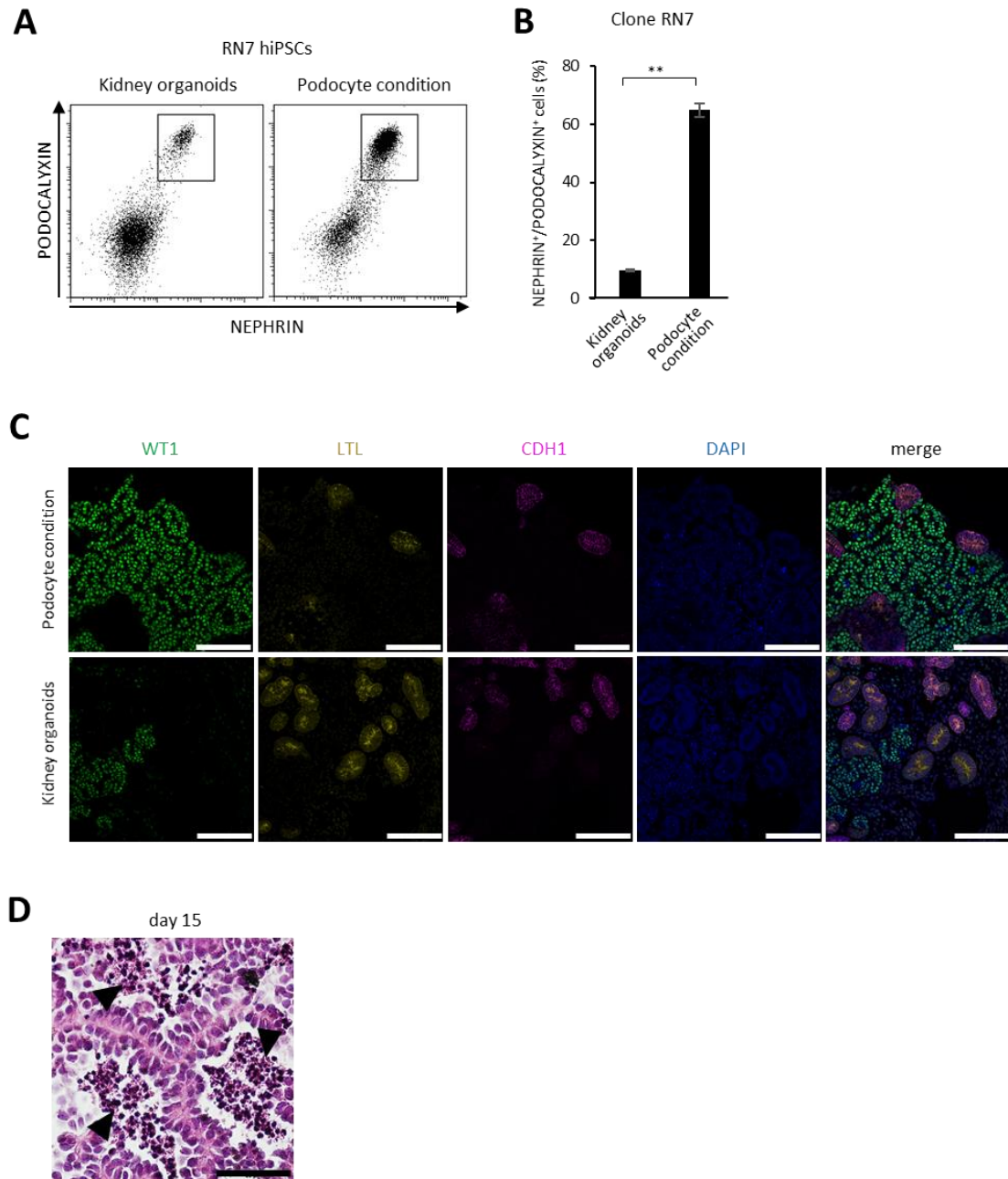
(n=3). N.D., not detected. (E) Immunostaining for pHH3, WT1 (proximal RV marker), and JAG1 (distal RV marker), and nuclear DAPI staining at 48 h in tissues cultured in each condition (n=3). Scale bars, 20 μ m. (F) Results of flow cytometry analyses at day 9 by modulating the concentration of SB after the proximalized RV step (STEP 3) (n=3). N.D., not detected. Data are shown as means \pm SEM.



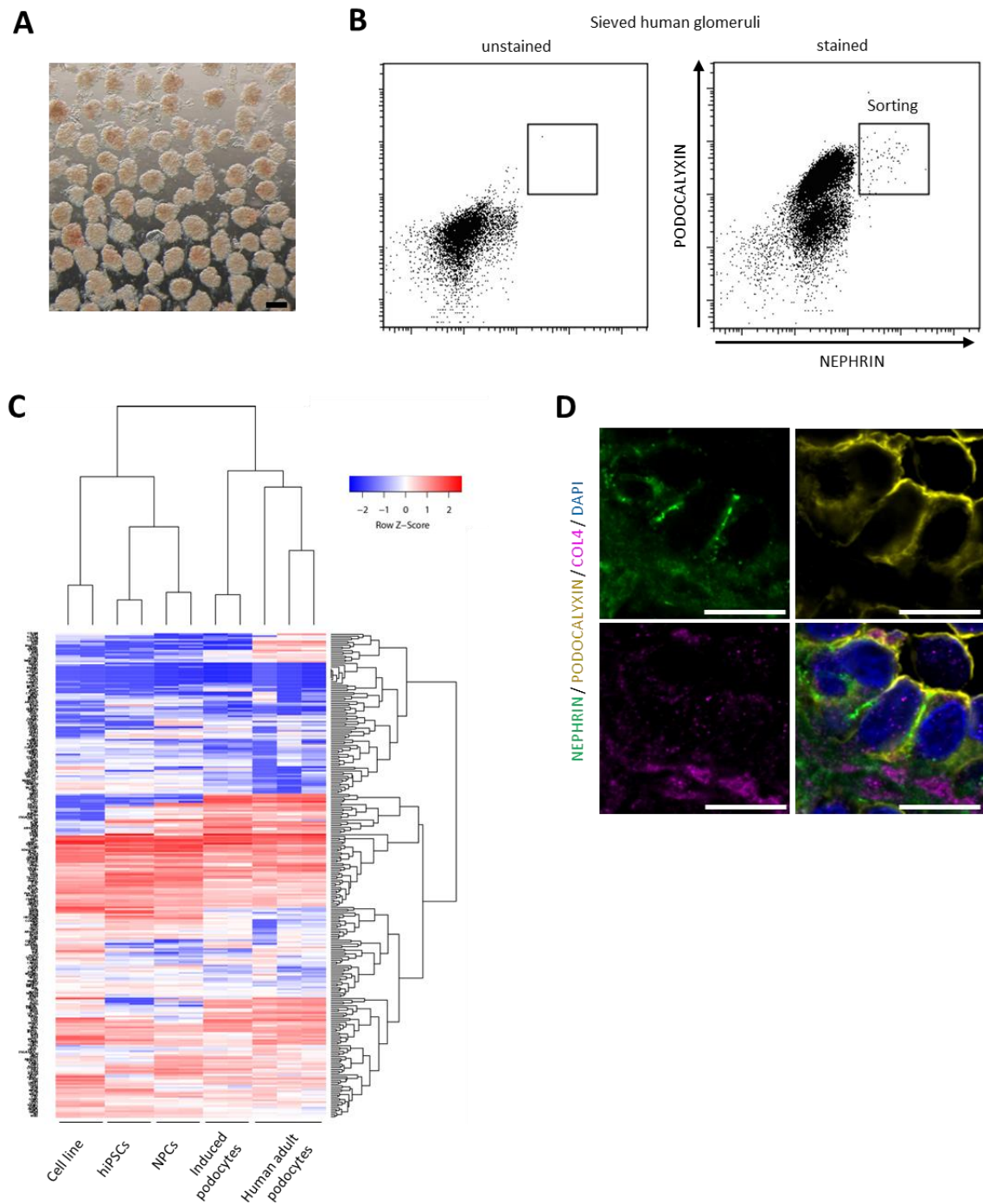
Supplemental Figure 7. Time-course analyses of differentiating cells in the podocyte induction protocol compared with the control protocol. (A) Schematic representation of the podocyte induction protocol compared with the control condition. (B, C) Immunostaining for pHH3, WT1 (podocyte precursor marker), JAG1 (proximal tubule precursor marker), and POU3F3 (distal tubule

(legend continued on next page)

precursor marker), and nuclear DAPI staining at day 6 in tissues cultured in each condition (B) as well as quantification of pHH3⁺ cells in each segment (C) (n=3). Scale bars, 20 μ m. (D, E) Immunostaining for WT1 (podocyte precursor marker), JAG1 (proximal tubule precursor marker), and POU3F3 (distal tubule precursor marker), and nuclear DAPI staining at day 6 in tissues cultured in each condition (D) as well as quantification of TUNEL⁺ cells by TUNEL assays in each segment (E) (n=3). Yellow arrowheads indicate TUNEL⁺ cells. Scale bars, 20 μ m. (F) Gene expression kinetics for podocyte (NPHS1, MAFB), proximal tubule (CDH6), and distal tubule (POU3F3) markers in each condition (n=3). (G) Histological sections stained with hematoxylin and eosin in each condition at day 9 (n=3). Blue arrowheads indicate PECs. Scale bars, 20 μ m. (H) Immunostaining for PODOCIN (podocyte marker) and PODOCALYXIN (podocyte and PEC marker), and nuclear DAPI staining in resultant cells in each condition at day 9 (n=3). White arrowheads indicate PECs (PODOCIN⁻/PODOCALYXIN⁺). Scale bars, 10 μ m. (I) Relative cell numbers of total cells and podocytes at day 9 in tissues in each condition (n=3). The podocyte number in the control condition was set as the baseline. Data are shown as means \pm SEM.



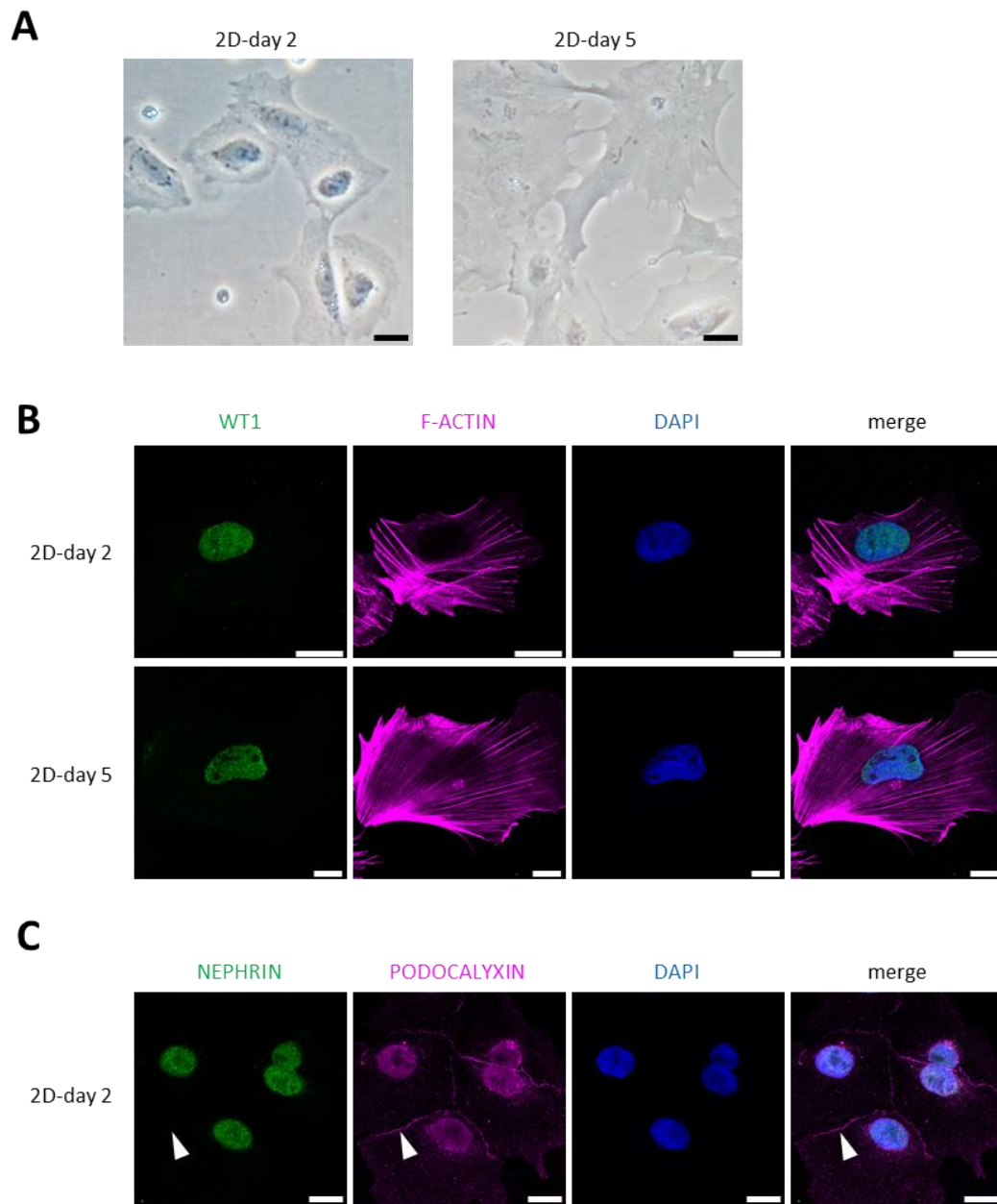
Supplemental Figure 8. Highly efficient podocyte induction from a separate integration-free iPSC line. (A, B) Flow cytometry analyses of NEPHRIN and PODOCALYXIN expression (A) and percentages of NEPHRIN⁺/PODOCALYXIN⁺ cells (B) at day 9 in kidney organoids and selectively induced podocytes from hiPSCs (RN7) (n=3). **P<0.01, Student's *t*-test. (C) Immunostaining for podocyte (WT1), proximal tubule (LTL), and distal tubule (CDH1) markers, and nuclear DAPI staining in resultant cells in each condition at day 9 (RN7) (n=3). Scale bars, 100 μ m. (D) Histological image of induced podocytes at day 15 stained with hematoxylin and eosin (n=3). The black arrowheads indicate regressed podocytes. Scale bar, 50 μ m. Data are shown as means \pm SEM.



Supplemental Figure 9. Procedure for isolating human adult podocytes and RNA-seq analysis of human podocytes. (A) Photograph of human glomeruli just after sieving from an adult kidney specimen (n=3). Scale bar, 200 μ m. (B) Flow cytometry analysis of sieved human glomeruli with anti-NEPHRIN and anti-PODOCALYXIN antibodies (n=3). The left and right panels show the results for unstained (negative control) and stained samples, respectively. Human adult podocytes were sorted as a NEPHRIN⁺/PODOCALYXIN⁺ population outlined by the black square in the right panel.

(legend continued on next page)

(C) Heatmap image and hierarchical clustering of RNA-seq analysis data using the podocyte-specific gene list published in Park et al.³⁹ Red, upregulation; blue, downregulation; cell line, conditionally immortalized human podocyte cell line cells (n=2); hiPSCs, undifferentiated hiPSCs (201B7) (n=2); NPCs, ITGA8⁺/PDGFRa⁻ NPCs induced from hiPSCs (n=2); induced podocytes, selectively induced podocytes from hiPSCs by our protocol (n=2); human adult podocytes, freshly sorted podocytes from human adult kidney (n=3). (D) Immunostaining for NEPHRIN, PODOCALYXIN, and COLLAGEN TYPE IV (COL4), and nuclear DAPI staining in induced podocytes at day 12 (n=3). Scale bars, 10 μ m.



Supplemental Figure 10. Extended two-dimensional culture of the induced podocytes. (A) Bright-field views of two-dimensionally cultured podocytes at day 2 and day 5. Scale bars, 20 μm . (B) Immunostaining for WT1 and F-ACTIN, and nuclear DAPI staining in two-dimensionally cultured podocytes at day 2 and day 5. Scale bars, 20 μm . (C) Immunostaining for NEPHRIN and PODOCALYXIN, and nuclear DAPI staining in two-dimensionally cultured podocytes at day 2. The white arrowheads indicate diminished NEPHRIN protein on the cell membrane. Scale bars, 20 μm .

Supplemental Table 1. Antibody Information

Antibody	Source	Catalog number	Analysis
Biotinylated Robo2	R&D	BAF3147	FC
anti-mouse Pdgfrb-APC	BioLegend	136008	FC
anti-mouse Podocalyxin-PE	MBL	D072-5	FC
Lhx1	DSHB	4F2	IHC
Cdh1	BD Biosciences	610181	IHC
Wt1	Abcam	ab89901	IHC, WB
DAPI	Sigma-Aldrich	D9542	IHC
Biotinylated LTL	VECTOR	B1325	IHC, FC
Cdh1-PE	BD Biosciences	562526	FC
Bio-ITGA8	R&D	BAF4076	FC
anti-human Pdgfra-PE	BioLegend	323506	FC
anti-human Podocalyxin	R&D	AF1658	IHC, FC
Jagged1	R&D	AF599	IHC
Pou3f3	Santa Cruz Biotechnology	sc-6028-R	IHC
pHH3	Abcam	ab14955	IHC
Nephrin	PROGEN	GP-N2	IHC
Nephrin (48E11)	(kindly provided by Dr. K. Tryggvason)		FC
Nephrin (C-term)	IBL	29070	WB
Nephrin (N-term)	IBL	29050	IEM
phospho-Nephrin	Abcam	ab80298	WB
Neph1	(kindly provided by Dr. Y. Harita)		IHC, WB
Podocin	IBL	29040	IHC, WB
Collagen Type IV	ROCKLAND	600-40-106-0.1	IHC
PLA2R	Abcam	ab211490	WB
GAPDH	Thermo Fisher Scientific	AM4300	WB
Phalloidin Alexa Fluor 594	Thermo Fisher Scientific	A12381	IHC
BV421 Streptavidin	BioLegend	405226	FC
APC Streptavidin	BioLegend	405207	FC
anti-mouse IgG1 PE	eBioscience	12401582	FC

Abbreviations: FC, flow cytometry; IHC, immunohistochemistry; WB, western blotting; IEM, immunoelectron microscopy.

Supplemental Table 2. Primer Sequences

Oligonucleotide		
Mouse	5'-Sequence-3' (forward)	5'-Sequence-3' (reverse)
b-Act	CATCCGTAAAGACCTCTATGCCAAC	ATGGAGCCACCGATCCACA
Six2	GCAACTTCCGCGAGCTCTAC	GCCTTGAGCCACAACCTGCTG
Pax2	AGGCATCAGAGCACATCAAATCAG	GGGTTGGCCGATGCAGATAG
Sall1	TGTCAAGTTCCCAGAAATGTTCCA	ATGCCGCCGTTCTGAATGA
Cited1	GTCGAGGCCTGCACTTGATG	CCAAGGTTGGAGTAGGCCAGAG
Robo2	GATCCAAGAGCCACGATCCAA	CCAGCACTGCACTCCAGGAA
Lhx1	AATGTAAATGCAACCTGACCGAGAA	GCGAACCAGATCGCTTGGA
Pax8	TTCTGCTATCGCAGGCATGG	AACTACAGATGGTCAAAGGCTGTGG
Cdh1	CACCGATGGTGAGGGTACACAG	GGCTTCAGGAATACATGGACAAAGA
Wt1	TGAAGACCCACACCAGGACTC	TGTGATGGCGGACCAATTC
MafB	GAGCTCCCATTGAGCCAAACA	ACACACTTGAGAGTTGCAGCGTTAG
FoxC2	TGTCAGCTGCCCTATCGAGCTA	ACAGCCTCAGTATTTGGTGCAGTC
Pou3f3	AACTGCACACTTGAGGTACTGTCCA	TCTTATCTCCGAGGCAGGTGTTC
Dkk1	GCCCAAGCAAGTGATTCCAGA	TTGGCTTAAGTTGGCAGGCTTC
Sox9	CAGGAAGCTGGCAGACCAGTA	AAGGGTCTCTTCTCGCTCTCGTT
Nphs1	AATTGGCGGCTGGGTCTTAG	TTTGTGTGGCATACACTGTCAGG
Nphs2	CTGTCTGCTACTACCGCATGGAA	CCCAAATACAGGTCCTGTCATCTAA
Cldn1	GATGTGGATGGCTGTCATTGG	CCATGCTGTGGCCACTAATGT
Lrp2	ACATCTGTATCTGCCATGTCACGTC	TGCCAGGCAAGGGTTGATTTA
Cdh6	CATAGGCTCTGTGCGAGCTCA	TTGTGCCACAGCAGGGTTTC
Human	5'-Sequence-3' (forward)	5'-Sequence-3' (reverse)
B-ACT	TGGCACCCAGCACAATGAA	CTAAGTCATAGTCCGCCTAGAAGCA
NPHS1	CAACTGGGAGAGACTGGGAGAA	AATCTGACAACAAGACGGAGCA
MAFB	TTGTAACCAGAATCACCTGAGGTC	CCAGGGTCAGGGATGGCTAA
CDH6	TTTACACAGCCACTGTCCCTGAA	CGTCGCAGTGACTTGGACAAC
POU3F3	CAGGGTGGACGATGCCTAAAG	AAGTTGGCAACGGATTGAGGA
NPHS2	GGAGGCTGAAGCGCAAAGAC	GCCATCCTCAGGGACTCAGAAG
WT1	AGGGTACGAGAGCGATAACCACAC	CTCAGATGCCGACCGTACAAGA
SYNPO	AAGTCACATCCAGTCTCTTC	CTTCTCCGTGAGGCTAGTG

Supplemental Methods

Flow Cytometry Analysis

Induced tissues were dissociated by incubation with 0.25% trypsin-EDTA for 8 min. The cell number in each sample was counted after dissociation. After blocking, primary antibody staining was carried out in 1× HBSS containing 1% bovine serum albumin and 0.035% NaHCO₃ for 30 min on ice, followed by secondary antibody staining for 10 min on ice. The stained cells were analyzed using a FACS CANTO II or a FACS SORP Aria (BD Biosciences).

qRT-PCR and RNA-seq

RNA was isolated with a RNeasy Plus Micro Kit (Qiagen) and reverse-transcribed with random primers using a Superscript VILO cDNA Synthesis Kit (Life Technologies). Quantitative PCR was carried out in a Dice Real Time System Thermal Cycler (Takara Bio) using Thunderbird SYBR qPCR Mix (Toyobo). The primer sequences are listed in Supplemental Table 2. All samples were normalized by β -actin expression. RNA isolated from hiPSCs (201B7), hiPSC-derived NPCs, hiPSC-derived podocytes, immortalized human podocyte cell line cells (two samples each), and three samples of human adult podocytes were subjected to RNA-seq analyses. Total RNA obtained from each sample was used for sequencing library construction with an Ovation Solo RNA-Seq System (NuGEN Technologies) according to the manufacturer's protocol. The quality of the libraries was assessed with an Agilent 2200 Tape Station High Sensitivity D1000 (Agilent Technologies). The pooled libraries for the samples were sequenced using a NextSeq 500 system (Illumina) in 76-bp single-end reads. For alignment to the whole transcriptome, sequencing adaptors, low-quality reads, and bases were trimmed with the Trimmomatic-0.32 tool.¹ The sequence reads were aligned to the human reference genome (hg19) using TopHat 2.1.1 (bowtie 2-2.2.3)² with the option '-g 1 --no-discordant'. NuDup ver.2.3 (NuGEN Technologies), which analyzes the redundancy of 8-bp molecular barcodes, was used to remove PCR duplicate reads. Files of the gene model annotations and known transcripts were downloaded from the Illumina iGenomes website (http://support.illumina.com/sequencing/sequencing_software/igenome.html), as required for whole transcriptome alignment with the TopHat software. For quantification of gene expression levels and detection of differentially expressed genes, the aligned reads were subjected to downstream analyses using StrandNGS 3.1 software (Agilent Technologies). The read counts allocated for each gene and transcript (RefSeq version 2015.10.5) were quantified using a Trimmed Mean of M-value (TMM) method.³ Hierarchical clustering of the differentially expressed genes was performed by R 3.5 package gplots (Ver. 3.0.1).

Immunohistochemical Analysis

Samples were fixed in 10% formalin, embedded in paraffin, and cut into 6- μ m sections. Antigen retrieval in pH 6.0 citrate buffer was performed before staining. The sections or cells were blocked with 1% bovine serum albumin (BSA) in PBS(–) for 60 min at room temperature, followed by

incubation with primary antibodies at 4°C overnight. Next, the sections were incubated with secondary antibodies conjugated to Alexa 488, 568, 594, 633, or 647 (Life Technologies) for 90 min at room temperature. Nuclei were counterstained with 4,6-diamidino-2-phenylindole (Roche). Fluorescence images were captured with a confocal microscope (TSC SP8; Leica). For quantification of proximal RV cells, differentiating tissues were dissociated by incubation with 0.25% trypsin-EDTA for 6 min and cytocentrifuged (Cytospin 2; Shandon), followed by immunostaining. Three randomly selected fields in each slide were captured with the TSC SP8 confocal microscope. The resulting images were processed and quantified with ImageJ, a public domain Java image processing program. TUNEL assays of the day 6 tissue were performed using ApopTag (Merck), and the signals were enhanced using the biotin-conjugated anti-dioxigenin antibody (Sigma-Aldrich) and Alexa 594 conjugated-streptavidin (Life Technologies). For quantification of pHH3⁺ and TUNEL⁺ cells, three randomly selected fields in each section were captured with the TSC SP8 confocal microscope. The resulting images were processed and quantified with ImageJ, a public domain Java image processing program. Detailed antibody information is provided in Supplemental Table 1.

Electron Microscopy

Transmission electron microscopy was performed as described.⁴ For immunoelectron microscopy, ultrathin cryosections were cut with an Ultracut UCT microtome (Leica) equipped with an FCS cryoattachment at -110°C as described,⁵ and then transferred to Formvar-coated nickel grids (150 mesh). After quenching of free aldehyde groups with PBS/0.01 M glycine, the sections were sequentially incubated with a primary antibody against the N-terminal domain of NEPHRIN overnight and a secondary antibody coupled to 12-nm gold particles (diluted 1:100 with PBS containing 10% fetal calf serum) for 60 min. Finally, the sections were fixed with 2.5% glutaraldehyde buffered with 0.1 M phosphate buffer (pH 7.4), contrasted with 2% neutral uranyl acetate solution for 30 min, and absorption-stained with 3% polyvinyl alcohol containing 0.2% acidic uranyl acetate for 30 min. The specimens were observed with a JEM1230 transmission electron microscope (JEOL). Detailed antibody information is provided in Supplemental Table 1.

Western Blot Analysis

Samples were lysed in RIPA buffer containing 25 mM HEPES-KOH (pH 7.8), 150 mM KCl, 1 mM MgCl₂, 1% Triton X-100, 1% sucrose, proteinase inhibitor cocktail, and phosphatase inhibitor cocktail (Sigma-Aldrich). The lysates were homogenized by ultrasonication on ice, and measured for their protein concentrations relative to a BSA standard using an Rc-protein Assay Kit (Bio-Rad Laboratories). The protein samples were denatured with 4× LDS sample buffer at 70°C for 10 min and electrophoresed in 4–12% Bis-Tris gels with MOPS buffer (Life Technologies). The separated proteins were transferred to PVDF membranes (Millipore), blocked with 5% nonfat dry milk in Tris-buffered saline containing 0.1% Triton X-100 (TBS-T), and incubated with primary antibodies at 4°C overnight. The membranes were washed with TBS-T, and incubated with horseradish peroxidase-conjugated

secondary antibodies. Bound antibodies were visualized with an ECL Select Western Blotting Detection Reagent (GE Healthcare) according to the manufacturer's instructions. Detailed antibody information is provided in Supplemental Table 1.

Two-Dimensional Culture of Induced Podocytes

Induced podocytes at day 9 were dissociated into single cells by incubation in Accutase (Merck) at 37°C for 8 min, and cultured two-dimensionally in DMEM/F12 supplemented with 5% FBS, 1% ITS, and 1% penicillin-streptomycin in a tissue culture chamber (SARSTEDT) coated with iMatrix-511 (Nippi). Cells were harvested at days 2 and 5. The harvested cells were washed once in PBS(–) and fixed with 2% paraformaldehyde for 5 min. After washing with PBS(–), the cells were permeabilized with 0.3% Triton X-100/PBS(–), followed by the immunohistochemical analyses described above.

Supplemental References

1. Bolger AM, Lohse M, Usadel B: Trimmomatic: a flexible trimmer for Illumina sequence data. *Bioinformatics* 30: 2114–2120, 2014
2. Langmead B, Salzberg SL: Fast gapped-read alignment with Bowtie 2. *Nat Methods* 9: 357–359, 2012
3. Robinson MD, Oshlack A: A scaling normalization method for differential expression analysis of RNA-seq data. *Genome Biol* 11: R25, 2010
4. Kurihara H, Harita Y, Ichimura K, Hattori S, Sakai T: SIRP- α -CD47 system functions as an intercellular signal in the renal glomerulus. *Am J Physiol Renal Physiol* 299: F517–527, 2010
5. Tokuyasu KT: Use of poly(vinylpyrrolidone) and poly(vinyl alcohol) for cryoultramicrotomy. *Histochem J* 21: 163–171, 19